Bulletin of the Seismological Society of America, Vol. 74, No. 3, pp. 805–818, June 1984

SOURCE MECHANISMS OF TWENTY-SIX LARGE, SHALLOW EARTHQUAKES ($M_S \geqq 6.5$) DURING 1980 FROM *P*-WAVE FIRST MOTION AND LONG-PERIOD RAYLEIGH WAVE DATA

BY ICHIRO NAKANISHI* AND HIROO KANAMORI

ABSTRACT

Source mechanisms of 26 large shallow earthquakes are determined in terms of a double-couple point source with a correction for the nondirectional part of source finiteness by using *P*-wave first motions and long-period Rayleigh wave spectra recorded on WWSSN, IDA, and GDSN networks. The combined use of both data sets allows us to determine the double-couple mechanism uniquely in most cases. Constrained linear moment tensor inversion ($M_{xz} = M_{yz} = 0$) correctly determines the strike of the fault, but fails to estimate the dip, and underestimates the scalar moment. All thrust events along the deep-sea trenches analyzed in this study show nodal planes which dip perpendicular to the trench axis at an angle shallower than 45°. The fit to data of the double-couple inversion is comparable to that of the constrained moment tensor inversion. Using the phase spectra of surface waves we can detect a slow source process with an accuracy of about 10 to 20 sec.

INTRODUCTION

The purpose of this study is to determine source mechanisms of 26 large shallow earthquakes which occurred during 1980. The earthquakes were analyzed by Kanamori and Given (1982) by applying a linear moment tensor inversion method (Kanamori and Given, 1981) to long-period Rayleigh waves. However, as noted by them, it is difficult or impossible to determine full moment tensor solutions of shallow earthquakes from long-period surface waves in the presence of complexities of the mantle and source process. To overcome the instability of the moment tensor solutions, Kanamori and Given (1982) constrained the two moment tensor elements, M_{xz} and M_{yz}, to be 0.

Many efforts have been made to retrieve moment tensor solutions from surface waves (e.g., Aki and Patton, 1978; Kanamori and Given, 1981) and free oscillations (e.g., Gilbert and Dziewonski, 1975; Mendiguren and Aki, 1978). Some attempts have been made to correct for lateral heterogeneity of the Earth only in an approximate way (Patton, 1980; Tréhu *et al.*, 1981; Romanowicz, 1981; Nakanishi and Kanamori, 1982).

For shallow events, the moment tensor solutions, especially the elements M_{xz} and M_{yz}, are very sensitive to the lateral heterogeneity and the complexity of the source process. The constrained linear moment tensor inversion used in Kanamori and Given (1982) is a robust approach to surface wave data, although it does not fully determine the source mechanism.

To determine M_{xz} and M_{yz} of shallow events, we need to analyze the higher frequency spectra of seismic waves. Dziewonski *et al.* (1981) and Dziewonski and Woodhouse (1983) applied normal mode theory to the body-wave part of long-period seismograms to obtain the full moment tensor solutions. They used a laterally homogeneous model of the Earth.

* Present address: Research Center for Earthquake Prediction, Faculty of Science, Hokkaido University, Sapporo 060, Japan.

Earthquakes occur in tectonically active regions, which have strong lateral heterogeneity. Lateral velocity variations as large as 5 to 8 per cent have been reported in island arc regions (Utsu, 1967; Oliver and Isacks, 1967). A similar heterogeneity beneath mid-oceanic ridges has been suggested from the nonorthogonality of nodal planes of the earthquakes on the ridge crests (Solomon and Julian, 1974). Since these heterogeneities are localized in the island arc and ridge regions, the long-period surface wave propagation is relatively unaffected by them. For example, Tréhu *et al.* (1981) showed that if they correct for the lateral heterogeneity by using regionalized phase velocities, the inversions of Rayleigh wave spectra lead to pure double-couple solutions for the earthquakes for which the first-motion data require nonorthogonal nodal planes. Thus, under certain circumstances, the use of surface waves can be more advantageous than the use of body waves to resolve source mechanism.

In the present study, we analyze the earthquakes using a double-couple point source. Although we make the constrained moment tensor inversions of surface wave data at a preliminary stage, we finally adopt the double-couple solutions. *P*-wave first motion data are added to the long-period Rayleigh wave data. An assumption in the combination of two data sets is that the initial break of an earthquake has the same focal mechanism as its main faulting. We will show that, at least for the shallow earthquakes analyzed here, the surface wave spectra can be fit by a double-couple source as consistently as by a moment tensor source. The *P*-wave first motions are generally consistent with the surface wave spectra.

Data

The source parameters of 26 earthquakes reported by National Earthquake Information Service (NEIS) are used in this study (Table 1). For many events, the source depths used by Kanamori and Given (1982) are adopted to calculate surface wave excitation.

P-wave first motions were read from the long-period, vertical component seismograms of WWSSN and GDSN (Engdahl *et al.*, 1982).

Long-period Rayleigh wave seismograms were retrieved from the magnetic tapes provided by IDA (Agnew *et al.,* 1976) and GDSN stations. The IDA seismograms have a sampling interval of 10 or 20 sec. We used the vertical component of the GDSN data. Original long-period GDSN seismograms have a sampling interval of 1 sec. We applied a low-pass filter with a cut-off period of 30 sec to the original seismograms and resampled them at an interval of 10 sec. The resampled records were analyzed together with the IDA data. The seismograms were windowed with fixed group velocities of 3.1 to 4.9, 3.3 to 3.9, 3.35 to 3.8, and 3.35 to 3.8 km/sec for R_1, R_2, R_3, and R_4, respectively. R_2 and R_3 were used in most cases. We did not use Love wave data. We made some experiments by incorporating them in source mechanism determination. However, inclusion of Love wave spectra, especially phase spectra did not improve the solutions. There may be two reasons for this. First, Love wave spectra do not resolve completely the moment tensor solution even in noise-free cases. Rayleigh waves have enough information to determine the moment tensor. Second, Love waves are more sensitive to lateral heterogeneity of the uppermost mantle than are Rayleigh waves. Considering these, we used only Rayleigh waves. Inclusion of Love waves would not lead to a major change in the solutions obtained in this study.

Using both IDA and GDSN networks, we obtain fairly complete azimuthal coverage of surface wave ray paths. For the Fox Island earthquake (no. 7 in Table

1), the coverage by the IDA network was too poor for Kanamori and Given (1982) to obtain its moment tensor solution. On the other hand, the GDSN network gives us good azimuthal coverage. For events in the New Hebrides (nos. 12, 13, 15, 16, 20, 21, and 22) and in Nepal (no. 17), the azimuthal coverage of the IDA network is superior to that of the GDSN. The coverage of well-operated stations became worse for the GDSN during 1981 (GDSN Newsletter, 1982). Thus, the combined use of both networks is desirable to obtain an unbiased estimate of source mechanism.

TABLE 1

LARGE SHALLOW EARTHQUAKES OF 1980

No.	Date (m	d)	Time (h	m	s)	Latitude (deg)	Longitude (deg)	Depth (km)	M_S	m_b	Region
1	1	1	16	42	40.0	38.815N	27.780W	10	6.7	6.0	Azores Island
2	1	2	20	58	44.2	5.984N	126.188E	63	—	6.0	Mindanao
3	2	7	10	49	16.0	54.158S	158.890E	10	6.5	6.1	Macquarie Island
4	2	23	5	51	3.2	43.530N	146.753E	44	7.0	6.3	Kurile Island
5	2	27	21	17	20.2	6.017S	150.189E	53	6.6	5.8	New Britain
6	3	8	22	12	10.3	22.673S	171.357E	38	6.7	6.1	Loyalty Island
7	3	24	3	59	51.3	52.969N	167.670W	33	6.9	6.2	Fox Island
8	6	9	3	28	18.9	32.220N	114.985W	5	6.4	5.6	Cal-Mex Border
10	6	18	17	14	54.5	9.475N	126.657E	54 (29)*	6.8	5.8	Mindanao
11	6	25	23	18	20.4	5.233S	151.686E	49	6.5	6.2	New Britain
12	7	8	23	19	19.8	12.410S	166.381E	33	7.5	5.9	Santa Cruz Island
13	7	9	20	56	53.2	12.689S	166.004E	33	6.7	5.2	Santa Cruz Island
14	7	14	16	15	1.7	29.273S	177.154W	49	6.6	5.8	Kermadec
15	7	17	19	42	23.2	12.525S	165.916E	33	7.9	5.8	Santa Cruz Island
16	7	29	3	11	56.3	13.101S	166.338E	48	6.7	5.9	Vanuatu Island
17	7	29	14	58	40.8	29.598N	81.092E	18	6.5	6.1	Nepal
18	9	26	15	20	37.1	3.225S	142.237E	33 (52)†	6.5	5.9	Papua
19	10	10	12	25	23.5	36.195N	1.354E	10	7.3	6.5	Algeria
20	10	24	3	25	34.4	21.989S	170.165E	33	6.7	5.8	Loyalty Island
21	10	25	7	0	7.9	21.982S	170.025E	33	6.7	5.7	Loyalty Island
22	10	25	11	0	5.1	21.890S	169.853E	33	7.2	5.8	Loyalty Island
24	11	8	10	27	34.0	41.117N	124.253W	19	7.2	6.2	North California
25	11	11	10	36	58.2	51.422S	28.796E	10	6.7	6.2	South off Africa
26	11	23	18	34	53.8	40.914N	15.366E	10	6.9	6.0	Italy
27	12	17	16	21	58.8	49.479N	129.496W	10	6.8	5.9	Vancouver Island
28	12	31	10	32	11.0	46.060N	151.453E	33	6.5	6.1	Kurile Island

* d = 29 km is reported by ISC.

† d = 52 km is reported by ISC.

ANALYSIS METHOD

Source process time. We first measure source process time by phase analysis of long-period Rayleigh waves (Furumoto and Nakanishi, 1983). The effect of the source finiteness is not serious for most of the earthquakes analyzed in this study. For the largest of the 26 earthquakes analyzed here, the phase delay due to the finite source process amounts to about 40 sec, which is equivalent to 1 radian for a period of 250 sec. If the effect were ignored in the linear moment tensor inversion, the scalar moment could be underestimated by a factor of 2. The measurement requires only an approximate knowledge of the origin time and epicentral location. An error in the origin time is absorbed in the measured source process time and does not affect the correction for the finite source process in the surface wave inversion. An epicentral mislocation error has no effect on the measurement.

The source process time in this paper is the nondirectional part of the apparent duration of the finite source process. For a horizontal unilateral fault (Ben-Menahem, 1961) the azimuthal variation of the apparent duration is the largest. For a symmetric bilateral fault (Aki, 1966), the azimuthal dependence of the phase shifts is weak. For L (fault length) = 100 km and V (rupture velocity) = 3 km/sec, the range of the azimuthal variation is estimated to be less than 0.1 sec. To obtain an accurate estimate of the directivity for each earthquake, we have to wait until detailed studies of aftershock distribution or finite source process are conducted by using local networks or near-field observations. The source process time itself, however, is insensitive to details of rupture mode (i.e., unilateral or bilateral).

The source process time is defined as a sum of delay time τ_D (delay of the main faulting from the initial break), rise time τ_R, and propagation time of the main rupture τ_L: $\tau = 2\tau_D + \tau_R + \tau_L$. The interpretation of τ in terms of τ_D, τ_R, and τ_L is not straightforward. Furumoto and Nakanishi (1983) made a statistical argument on the interpretation of τ for shallow-angle thrust events along deep-sea trenches. A primary purpose of measuring τ in this study is to correct for the nondirectional part of the finite source process. To do this we need not separate the three terms (Nakanishi and Kanamori, 1982).

Moment tensor solution with constraint. Using the source process times derived from the phase analysis, we invert long-period (256-sec) Rayleigh wave complex spectra to determine the parameters of the constrained ($M_{xz} = M_{yz} = 0$) moment tensor source. We use a linear inversion method described in Kanamori and Given (1981). The results are in good agreement with those of Kanamori and Given (1982), except for event 7, which was not analyzed by them. The moment tensor solutions are decomposed into two double-couples. The strike and the scalar moment of the major double-couple will be used to obtain a mechanism solution which is consistent with both surface wave and P-wave first motion data. Some events, especially events 18 and 25, have a large second double-couple. For these events, we pay special attention when we interpret the Rayleigh wave spectra using a single double-couple. As will be shown later, a single double-couple can explain satisfactorily the Rayleigh wave radiation patterns of these events.

The constrained moment tensor solution is a best fit to the data under the constraints $M_{xx} + M_{yy} + M_{zz} = M_{xz} = M_{yz} = 0$. The goodness of fit can be expressed by the rms of the difference between the observed and calculated source spectrum (both the real and imaginary parts). Changing M_{xz} and M_{yz} from 0 has little effect on rms (for this reason M_{xz} and M_{yz} are indeterminate), yet it changes the mechanism significantly. Mechanism solutions whose rms value is approximately equal to that of the constrained moment tensor are considered consistent with the surface-wave data.

In combining surface-wave and first-motion data, we search for a double-couple solution that is consistent with the P-wave data, while keeping track of the ratio of the rms for the double-couple solution to that for the constrained moment tensor. If a solution for which the ratio is approximately 1 is found, we conclude that the source can be adequately represented by a double-couple; if not, some non-double-couple component is required. The actual procedure is different for different events, depending upon the mechanism (strike slip vs. dip slip), and the azimuthal distribution of the first-motion data.

Nodal plane determination from P-wave polarity. The polarities of P-wave first motion are classified as up, down, or nodal, and used to constrain one of the nodal planes before the double-couple inversion is performed.

For strike-slip events (nos. 1, 3, 8, 24, and 27), *P*-wave first motion data usually determine the two nodal planes which are consistent with the Rayleigh wave radiation pattern. In some cases we need a small modification.

For thrust events along the trenches, the dip of the steeply dipping nodal plane is determined almost uniquely from the *P*-wave data if we constrain the strike based on the constrained moment tensor solution obtained in the previous step. These are events nos. 2, 4, 5, 6, 7, 10, 11, 12, 13, 14, 15, 16, 20, 21, 22, and 28. For event 18 (Papua) the constrained moment tensor has a large minor couple (38 per cent of major couple), and the strike direction of the major couple is inconsistent with the *P*-wave first motions. For this event, we discard the constrained solution and adopt one nodal plane well constrained by the *P*-wave first motions for the next step of this analysis.

For two intraplate events (nos. 19 and 26), one of the nodal planes is constrained by the *P*-wave first motion data. For an event in Nepal (no. 17), there remains an ambiguity of the dip even if we constrain the strike of the nodal plane based on the Rayleigh wave radiation.

A normal-fault event on the Prince Edward West Fracture Zone (no. 25) shows a large minor double-couple (42 per cent of major couple). The coverage of the focal sphere by *P*-wave first motion data is not good enough to constrain either one of the nodal planes. We have to make a trial and error search to find a solution consistent with both *P*-wave first motion and Rayleigh wave radiation pattern. We will discuss this earthquake later in some detail.

Double-couple inversion of Rayleigh wave spectra. As the final step, a double-couple point source solution [strike φ, dip δ, slip (rake) λ, seismic moment M_0] is determined by the inversion of Rayleigh wave spectra by fixing two or three of the four parameters. Rayleigh wave spectrum is a nonlinear (trigonometric) function of φ, δ, and λ. We use an iterative nonlinear inversion method suggested by Kanamori and Given (1981). In many cases, λ and M_0 are made free and are determined. We attempted the inversions in which φ, δ, or both were made free, but generally the iterations did not converge to a solution consistent with the *P*-wave first motion. Therefore, we adopt the result with fixed φ and δ as a final mechanism solution of this study.

Results

Table 2 presents the results. In Figure 1 (a to e), the solutions of the constrained double-couple inversions are compared with the *P*-wave first motion data. Twelve of the 26 earthquakes have been analyzed for source mechanisms and seismic moments by different authors. These studies are listed in Table 2. Our solutions are in good agreement with the results of these authors. The solutions presented in Table 2 are explained in detail in the following.

Source process time. The standard deviations of the measured source process times ($\Delta\tau$) are generally independent of the seismic moment, because the accuracy relies upon the accuracy of the great circle phase difference. A mean value of $\Delta\tau$ of Table 2 is 17 sec. Furumoto and Nakanishi (1983) obtained a similar value as a standard error of the source process times measured by them. This error estimate must be kept in mind when interpreting the measured source process times in terms of the finite source process.

Two events exhibit a source process time much longer than that expected from their size (M_S or M_0). One is an event in the Santa Cruz Island (no. 13), and the other occurred in Italy (no. 26).

Nakanishi and Kanamori (1982) also obtained an anomalously long source process time for the Santa Cruz Island earthquake (no. 13). Another seismological evidence supports the slow source process. The event 13 has $M_S = 6.7$ and $m_b = 5.2$ (Table 1). Large Santa Cruz Island events also show large discrepancies between M_S and m_b (no. 12, $M_S = 7.5$, $m_b = 5.9$; no. 15, $M_S = 7.9$, $m_b = 5.8$). If we take into account the saturation of m_b around 6.0 (Geller, 1976), the $M_S - m_b$ disproportionality of

TABLE 2

SOURCE PROCESS TIMES (WITH STANDARD DEVIATIONS), FOCAL SOLUTIONS, AND SEISMIC MOMENTS

No.	τ (sec)	$\Delta\tau$ (sec)	ϕ_1 (deg)	δ_1 (deg)	λ_1 (deg)	ϕ_2* (deg)	δ_2* (deg)	M_0 (10^{27} dyne-cm)	d (km)	DC/MT†	Ref.‡
1	17	14	−31	86	3	239	87	0.24	9.75	0.99	a
2	35	17	6	64	85	−163	26	0.45	62.0	1.35	
3	30	18	−70	84	0	20	90	0.19	9.75	1.19	
4	19	19	27	70	89	−151	20	0.63	43.0	1.09	
5	27	3	88	60	92	−96	30	0.21	53.0	1.10	
6	44	27	117	66	89	−61	24	0.61	33.0	1.03	
7	30	27	53	60	88	−123	30	0.30	33.0	1.01	
8	15	3	140	90	180	50	90	0.047	9.75	1.02	b
10	26	14	6	82	92	−188	8	0.49	33.0	1.35	
11	16 (49)§	—ˆ	70	52	92	247	38	0.086	43.0	0.99	
12	51	18	170	59	93	−16	31	2.15	33.0	1.02	c, d
13	41	14	166	64	90	−14	26	0.17	33.0	1.03	b, c, d
14	18	7	10	70	83	−150	21	0.14	43.0	1.23	
15	83	12	166	52	90	−14	38	6.44	33.0	0.97	c, d
16	19	19	160	54	94	−26	36	0.16	43.0	1.00	b
17	15	21	111	70	90	−69	20	0.083	16.0	0.99	
			111	50	90	−69	40	0.054	16.0	0.99	
18	14	15	−4	72	129	107	42	0.17	53.0	1.21	
19	30	21	225	54	82	59	37	0.49	9.75	1.06	e, f, g, n
20	26	16	140	68	90	−40	22	0.24	33.0	1.04	h
21	39	6	143	74	93	−48	16	0.93	33.0	1.20	h
22	47	13	142	73	88	−32	17	2.92	33.0	1.07	h
24	32	19	50	90	0	140	90	1.03	16.0	1.00	i, j, k
25	28	18	−137	78	248	−65	155	0.32	9.75	1.02	
			−150	78	243	−82	150	0.32	9.75	1.00	
26	45	13	−43	63	276	−56	152	0.28	9.75	1.00	l, m
27	26	11	−37	90	180	53	90	0.15	9.75	1.02	
28	28	13	28	68	90	−152	22	0.29	33.0	0.98	

* ϕ_2 and δ_2 are presented for convenience. Use (ϕ_1, δ_1, λ_1), which is determined in this study, for any purposes.

† Ratio of rms residuals between double-couple and moment tensor inversion. DC, double-couple inversion; MT, constrained moment tensor inversion.

‡ a, Hirn *et al.* (1980); b, Nakanishi and Kanamori (1982); c, Tajima and Kanamori (1982); d, Tajima (1982); e, Deschamps *et al.* (1982); f, Ouyed *et al.* (1981); g, Cisternas *et al.* (1982); h, Vidale and Kanamori (1981); i, Eaton (1981); j, Smith *et al.* (1981); k, Lay *et al.* (1982); l, Boschi *et al.* (1981); m, Del Pezzo *et al.* (1983); n, Ouyed *et al.* (1983).

§ $\tau = 16$ sec is calculated from an empirical formula. $\tau = 49$ sec is measured from ESK.

ˆ One measurement is available.

events 12 and 15 may be due to the size of the earthquakes. On the other hand, event 13 seems to be too small to reach the m_b saturation. An earthquake in the Vanuatu Island region (no. 16), which is close to the Santa Cruz Island, has a similar M_S, but does not show the large $M_S - m_b$ difference ($M_S = 6.7$, $m_b = 5.9$). The disproportionality may be related to the slow source process of event 13. Many of the P-wave first motions from this event are not as clear as those from events 12, 15, and 16, suggesting that at least the initiation of event 13 was slow.

The Irpinia earthquake (no. 26) also shows a long source process time of 45 sec. Boschi *et al.* (1981) obtained a large origin time perturbation of 17 sec by applying the method of Dziewonski *et al.* (1981) to IDA and GDSN data, and inferred the event to be multiple. The above origin time shift is approximately equivalent to a source process time of 34 sec by our definition. Considering the difference between the two methods, the two estimates of source duration are in good agreement.

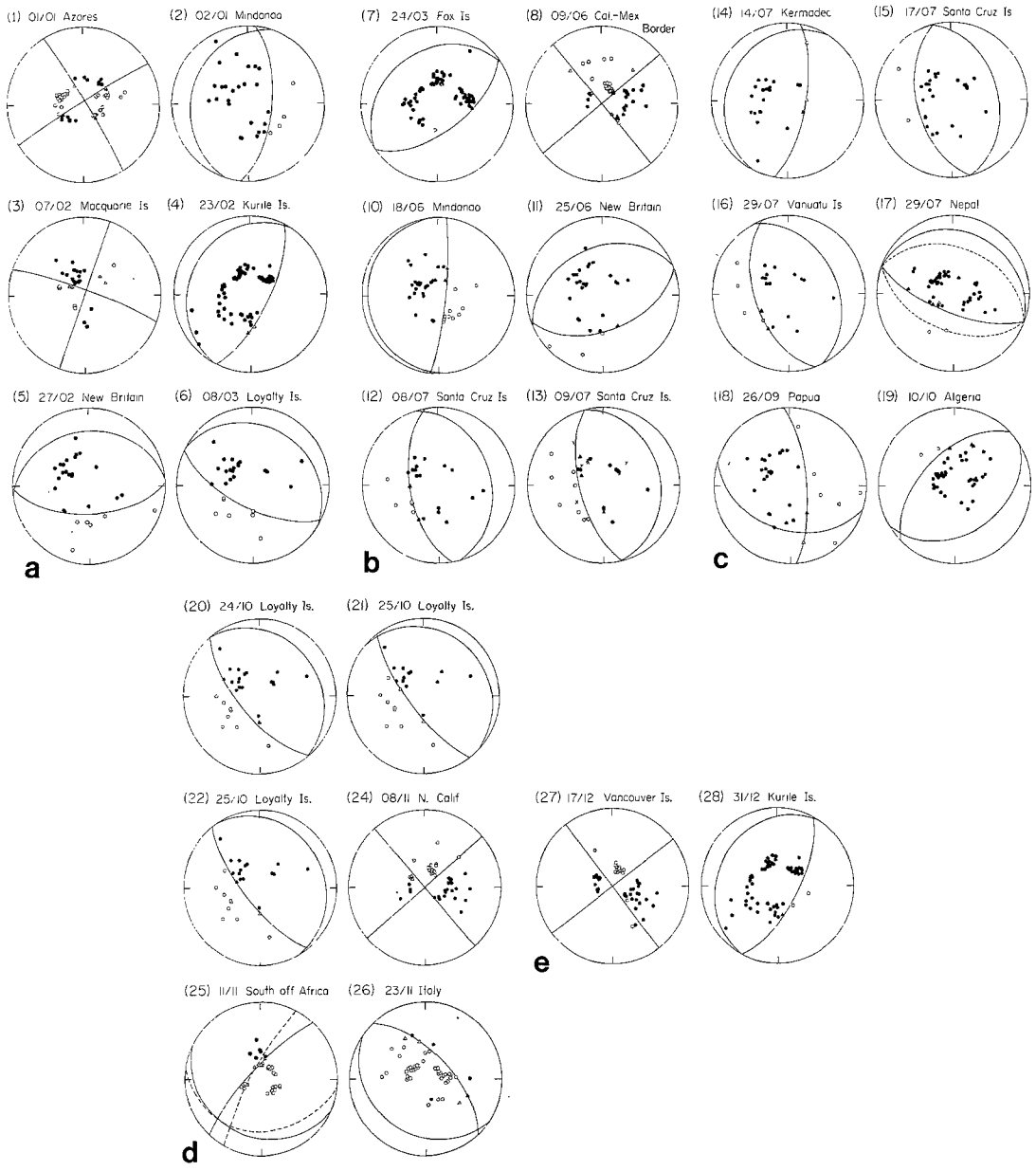

FIG. 1. Focal mechanism solutions (Table 2) compared with the observed *P*-wave first motions. Lower hemisphere equal area projection is adopted. Solid and open symbols indicate "up" and "down" *P*-wave first motions on the vertical component seismograms, respectively. Circle indicates a clear *P*-wave onset. Triangle means that the *P*-wave first motion possesses a nodal character. The same numbering as in Tables 1 and 2 is adopted here. For event 13, the data which were read but not used to constrain the solution are represented by *x*. In the diagram for event 17, two solutions are shown for $\delta =$ 70° and 50° by solid and dashed lines, respectively. For event 25, two nodal planes are shown by solid and dashed lines. See text for details.

Double-couple point source. In the following we briefly comment on each of the double-couple solutions.

Azores Island (no. 1): Double-couple solution of this earthquake is determined uniquely from the P-wave first motion and is in good agreement with the Rayleigh wave radiation pattern. The P-wave polarities suggest a nearly vertical fault ($\delta_1 = 86°$ or $\delta_2 = 87°$). Hirn *et al.* (1980) conducted a detailed observation of the aftershock sequence of this event. Although they did not study the main shock, they obtained an aftershock distribution and a composite mechanism solution of the aftershocks. The composite solution exhibits a slight counterclockwise rotation of the strike with respect to our solution. The aftershock distribution is in good agreement with one of the nodal planes of our solution ($\varphi_1 = -31°$ and $\delta_1 = 86°$).

Mindanao (no. 2): The steeply dipping nodal plane of this event is not well constrained by the P-wave first motions. However, fixing the strike of the nodal plane ($\varphi = 6°$) based on the result of the constrained moment tensor inversion, we can almost uniquely determine the dip ($\delta = 64° \pm 4°$) from the P-wave first motions. The other nodal plane or λ and M_0 are determined by the double-couple inversion of Rayleigh wave spectra.

Macquarie Island (no. 3): For this event, we fix the strike of one nodal plane ($\varphi = -70°$) based on the constrained moment tensor inversion and determine the dip ($\delta = 84° \pm 2°$) from the P-wave first motions. For vertical ($\delta = 90°$) strike-slip events, the long-period Rayleigh wave spectrum becomes $U \propto M_0 \cos \lambda \sin 2\varphi$, where φ is the azimuth of the station measured counterclockwise from the strike. Thus, λ becomes indeterminate. We fix $\lambda = 0°$ and determine M_0.

Kurile Island (no. 4): The steeply dipping nodal plane is constrained uniquely ($\varphi = 27° \pm 3°$ and $\delta = 70° \pm 1°$) from the moment tensor inversion and P-wave polarities.

New Britain (no. 5): We fix the strike of the steeply dipping nodal plane to be 88° based on the constrained moment tensor inversion. With this constraint the P-wave polarities lead to $\delta = 60° \pm 3°$.

Loyalty Island (no. 6): Based upon the solution of the constrained moment tensor inversion, we constrain $\varphi = 117°$ and obtain $\delta = 66° \pm 1°$ from the P-wave data.

Fox Island (no. 7): Even if we constrain the strike ($\varphi = 53°$), there remains an ambiguity in δ. We choose the steepest allowable dip. Since some stations close to this nodal plane exhibit a nodal character, the error in δ may be small.

California–Mexico Border (no. 8): From the P-wave first motions, we can constrain the two nodal planes ($\varphi_1 = -45°$, $\delta_1 = 90°$; $\varphi_2 = 45°$, $\delta_2 = 90°$). However, the Rayleigh wave radiation requires a slight clockwise rotation of the nodal planes ($\varphi_1 = -40°$). The new nodal planes are consistent with the P-wave polarities, because many stations near the nodal lines show nodal characters. Constraining φ_1, δ_1, and λ_1, we obtain $M_0 = 0.047 \times 10^{27}$ dyne-cm.

Mindanao (no. 10): First we used a source depth of 53 km based on the NEIS solution. With this depth, we could not find a double-couple solution that could explain both P-wave first motions and Rayleigh wave spectra. Since ISC reports a depth of 29 km for this event, we use a point source depth of 33 km and find a solution which is consistent with both data sets. We fix φ to be 6° and obtain $\delta = 82° \pm 1°$ from the P first motions.

New Britain (no. 11): Fixing $\delta = 70°$, we obtain $\delta = 52° \pm 1°$ from the P-wave data. For this event, we obtained a single measurement of τ of 49 sec from (R_2, R_3, R_4) observed at ESK. However, this value seems to be too long as a source process time of this event. If we use this value, we have a systematic phase advance in the

initial phases equalized back to the epicenter. A small difference of 0.3 between M_S and m_b is also a negative evidence against the long source process. We use $\tau = 16$ sec, which is calculated from an empirical relation between τ and M_0 proposed by Furumoto and Nakanishi (1983), in the moment tensor and double-couple inversions of Rayleigh wave spectra.

Santa Cruz Island (no. 12): The steep nodal plane is determined uniquely ($\varphi = 170° \pm 1°$; $\delta = 59° \pm 1°$) from the P-wave first motion data.

Santa Cruz Island (no. 13): The P-onsets from this event are generally unclear. It is not easy to assign up or down for several stations. Since such stations are close to the stations that show relatively clear onsets on the focal sphere, we disregard those observations in the determination of nodal plane. The disregarded stations are represented by x in Figure 1. The constrained moment tensor inversion gives $\varphi = 166°$. Using this value we obtain $\delta = 64° \pm 3°$ from the first motions.

Kermadec (no. 14): We constrain $\varphi = 10°$ and obtain $\delta = 70° \pm 1°$ from the P-wave data. The constrained moment tensor inversion requires $\varphi = 18°$. We take the above value so as to be consistent with the P-wave polarities as well as possible.

Santa Cruz Island (no. 15): Even if we constrain the strike, the dip is not determined uniquely from the P-wave polarities. We adopt tentatively $\delta = 52°$. The polarity data permit δ to vary from 38° to 55°. Since $\delta = 46° \pm 9°$, the uncertainty has only a small effect upon the estimate of M_0.

Vanuatu Island (no. 16): We fix φ to be 160° and obtain $\delta = 54° \pm 1°$ from the P-wave polarities. If we make φ to be free, we have $\varphi = 160°$ to 180° and $\delta = 54°$ to 60°.

Nepal (no. 17): The constrained moment tensor inversion gives $\varphi = 111°$. Even if we fix the strike at this value, the dip is not uniquely determined ($\delta = 50°$ to 70°). Since a few stations exhibit a nodal character, the actual dip of the nodal plane seems to be close to 70°. Considering the absence of strong evidence for $\delta \approx 70°$, we present two focal solutions for $\delta = 50°$ and $\delta = 70°$ in Table 2 and in Figure 1. As the table shows, the seismic moment is uncertain by a factor of 1.6.

Papua (no. 18): The constrained moment tensor inversion gives a solution with a large minor couple (38 per cent of the major couple), and the strike direction of the major couple is inconsistent with the P-wave first motions. We discard the constrained solution and adopt one nodal plane which is well constrained by the P-wave first motions: $\varphi = -4° \pm 4°$; $\delta = 72° \pm 4°$. Starting from $\lambda = 90°$, $\varphi = -4°$, $\delta = 72°$, and $M_0 = 0.14 \times 10^{27}$ dyne-cm, the double-couple inversion converges to the solution shown in Table 2 and Figure 1. The solution has a significant oblique-slip component ($\lambda = 129°$). We use 53 km as a source depth based on the value reported by ISC.

Algeria (no. 19): This event (the El Asnam earthquake) has been extensively studied by French and British scientists. They conducted detailed studies of the main shock by means of body and surface wave analyses (Deschamps *et al.*, 1982) and detailed geological and geophysical surveys of the faulted region including aftershock observations (King and Vita-Finzi, 1981; Ouyed *et al.*, 1981, 1983; Cisternas *et al.*, 1982). Our polarity data do not constrain the nodal plane ($\varphi = 184°$ to 254°; $\delta = 48°$ to 66°). We adopt a nodal plane ($\varphi = 225°$ and $\delta = 54°$) obtained by Deschamps *et al.* (1982) for the constraint in the double-couple inversion of Rayleigh wave spectra.

Loyalty Island (no. 20): The constrained moment tensor inversion gives $\varphi = 140°$. With this strike, we obtain $\delta = 57°$ to 69° from the P-wave data. Considering the two nodal stations, we choose $\delta = 68°$.

Loyalty Island (no. 21): The P-wave polarities constrain a nodal plane ($\varphi = 143° \pm 2°$; $\delta = 74° \pm 1°$).

Loyalty Island (no. 22): The P-wave first motions constrain $\varphi = 136°$ to $142°$ and $\delta = 72°$ to $74°$. The constrained moment tensor inversion results in $\varphi = 144°$. We constrain $\varphi = 142°$ and $\delta = 73°$ in the double-couple inversion.

Northern California (no. 24): The main shock and its aftershocks were located by Eaton (1981) and Smith *et al.* (1981) by using local networks. The events occurred on a plane which strikes about N50°E. The constrained moment tensor inversion leads to a vertical nodal plane which strikes N50°E. This solution is shown in Table 2 and Figure 1. M_0 is determined by the constrained double-couple inversion.

South off Africa (no. 25): The solution of the constrained moment tensor inversion shows a large minor double-couple (42 per cent of major couple). The major couple strikes $\varphi = -110°$. Constraining the strike to this value we have $\delta = 71°$ from the P-wave polarities. However, with these values of φ and δ, we cannot find a solution consistent with Rayleigh wave phase spectra. After a trial-and-error search we find that $\varphi = -137°$, and $\delta = 78°$ leads to a solution that explains the phase spectra. The nonlinear inversion leads to $\lambda = 248°$ and $M_0 = 0.32 \times 10^{27}$ dyne-cm. As Figure 1 shows, this solution (solid line) is consistent with the P-wave first motion data. The surface wave radiation, however, requires a slight counterclockwise rotation of the steep nodal plane, which appears to be inconsistent with some of the first motions close to the nodal line. The double-couple solution that well explains the surface wave spectra is also listed in Table 2 and is shown by the dashed line in Figure 1. The latter solution is more consistent with the strike of the Prince Edward West Fracture Zone, than the former solution.

Italy (no. 26): The P-wave polarities uniquely constrain a steep nodal plane ($\varphi = -43°$; $\delta = 63°$).

Vancouver Island (no. 27): The P-wave first motion data do not constrain the nodal planes well. The constrained moment tensor inversion results in $\varphi = -37°$, $\delta = 90°$, and $\lambda = 180°$. We constrain $\lambda = 180°$ and determine M_0.

Kurile Island (no. 28): The P-wave polarities require $\varphi = 41°$ to $18°$ and $\delta = 68°$ to $70°$. The constrained moment tensor inversion leads to $\varphi = 28°$. If we adopt this strike we have $\delta = 68° \pm 2°$.

Discussion

Deviation from the double-couple. The moment tensor is a more general earthquake source than the double-couple. If we assume no isotropic component, the moment tensor can be decomposed into two double-couples (Gilbert, 1981).

Kanamori and Given (1982) and Dziewonski and Woodhouse (1983) reported that some earthquakes have significantly large minor (second) double-couples. Kanamori and Given obtained large minor double-couples [larger than 20 per cent of the major (first) double-couple] for events 3, 5, 8, 18, 25, and 27 of the present study. Although they pointed out several possible sources of the large minor double-couples, they tentatively assumed that the earthquake mechanism is a single double-couple and that the minor double-couple is an artifact of the constraint $M_{xz} = M_{yz} = 0$. Dziewonski and Woodhouse discussed the dependence of the deviations from the double-couple on the seismic moment, the focal depth, and the geographic position, and concluded that earthquakes in some regions, for example shallow earthquakes along the northern coast of New Guinea, produced large deviations from the double-couple.

We assume the double-couple mechanism to analyze the P-wave first motions and the Rayleigh wave spectra in this paper. The moment tensor inversion is made only to obtain an initial solution with the constraint $M_{xz} = M_{yz} = 0$. Some earthquakes, especially events 18 and 25, show considerable minor double-couples. We obtain 38 and 42 per cent minor double-couples for events 18 and 25, respectively. However, we find that the double-couples with a significant amount of oblique slip can explain well the Rayleigh wave spectra that require the large minor double-couples if we assume $M_{xz} = M_{yz} = 0$. The obtained double-couple solutions are consistent with the P-wave first motions, as can be seen in Figure 1.

To make a quantitative comparison between the double-couple (DC) and the constrained moment tensor (MT) inversions, we compute the ratio of rms residuals of the inversions. They are listed in Table 2. The ratio DC/MT is 1.02 or 1.00 for event 25, for which the largest minor double-couple (42 per cent) is obtained from the constrained moment tensor inversion. This suggests that for at least this event, the large minor double-couple is an artifact caused by the large oblique slip and the constraint $M_{xz} = M_{yz} = 0$. For event 18, the ratio is 1.21, indicating that the data can be fitted considerably better by the constrained moment tensor than by the double-couple.

TABLE 3

FOCAL SOLUTIONS AND SEISMIC MOMENTS DERIVED FROM EXTENDED SOURCES*

No.	φ_1 (deg)	δ_1 (deg)	λ_1 (deg)	M_0 (10^{27}dyne-cm)	d_M† (km)	DC/MT‡	
2	6	64	88	0.36	66.5	1.15	(1.35)‡
10	6	82	93	0.54	38.0	1.17	(1.35)
14	10	70	84	0.12	38.0	1.05	(1.23)
18	−4	72	126	0.15	48.0	1.04	(1.21)
21	143	74	94	0.85	38.0	1.08	(1.20)

* Excitation functions are calculated for distributed sources that extend from 0 to d_M. The definition of the excitation functions is given by equation (20) of Kanamori and Given (1981).

† τ are the same as in Table 2.

‡ DC, double-couple inversion; MT, constrained moment tensor inversion. The values in parentheses are taken from Table 2.

Table 2 contains the DC/MT ratios for the 24 other earthquakes. Except for several events, the goodness of fit is comparable for both inversions, which means that the moment tensor is not necessary to interpret the Rayleigh wave spectra.

Point source depth for long-period surface wave excitation. Events 2, 10, 14, 18, and 21 show DC/MT ratios larger than 1.2 (Table 2). We notice that these events have relatively deep source depths determined by P-wave arrivals (NEIS and ISC). One event in Mindanao (no. 2), which has DC/MT = 1.35, is the deepest of the 26 earthquakes studied here. For the five events, we investigate the effect of an extended source upon the surface wave inversion. We assume a source extending from a depth 0 to d_M. We use excitation functions calculated by Kanamori and Given (1981). We assume that the initial break of the earthquake, which is located by the short-period P-wave arrivals, occurred at d_M and that the rupture extended over a depth range from d_M to 0. Table 3 presents the inversion results obtained by using the extended sources. The focal solutions of this table differ only slightly from those of Table 2. We notice reduction of DC/MT ratios in Table 3. The reduction varies from 0.12 to 0.2 in the five cases. The deepest event, no. 2, shows the largest reduction of DC/MT ratio. Our experiment shows that some parts of

the residuals in the constrained double-couple inversions can be explained by an extended source. This may suggest that the point source depths for the long-period surface wave radiation (centroid) are shallower than those located by the short-period P-arrivals for these events.

Effect of lateral structural heterogeneity on the P-wave first motion pattern. It is possible to reduce the DC/MT ratios by changing the constraints on φ, δ, and λ of one or two nodal planes which were used in the double-couple inversions.

Toksöz *et al.* (1971) and Solomon and Julian (1974) studied the distortion of the radiation pattern due to the localized lateral heterogeneity in the subduction zone and oceanic ridge, respectively, by using a ray tracing technique (Julian, 1970). Solomon and Julian explained the observed nonorthogonality of P-wave first motions from the ridge-crest earthquakes by the laterally heterogeneous mantle beneath the ridge. Although it is not obvious whether their argument applies to every subduction and every ridge earthquake, we may have to keep in mind the possible distortion of the radiation pattern when analyzing the first motion data. Part of the inconsistency between the body-wave data and surface-wave data might be explained by lateral heterogeneity in the epicentral region. Of course the argument of this paper does not rule out the possible deviations of source mechanism from the double-couple. It will not be easy to interpret the apparent second double-couple until the corrections for the local and global lateral heterogeneity can be made to the first motion and the surface wave data.

Conclusions

1. Double-couple point source mechanisms of 26 large shallow earthquakes are determined by the combined use of P-wave first motion and Rayleigh wave data.
2. The P-wave first motion data do not always constrain the nodal planes uniquely. The combined use of surface-wave radiation pattern significantly reduces the nonuniqueness.
3. For thrust earthquakes along the trenches, the constrained moment tensor solutions determine the overall strike direction, but the dip angle is inconsistent with that inferred from the P-wave first motions for the steeply dipping nodal plane. The error in the dip angle systematically underestimates the scalar moment.
4. The double-couple source can explain the surface-wave data as well as the constrained moment tensor source does. The Rayleigh waves from two earthquakes, which produce large minor double-couples (about 40 per cent of the major double-couple) in the constrained moment tensor inversion, can be interpreted by a single double-couple with a large oblique slip component.
5. The source process times measured by the phase spectra can be used to detect anomalous source processes, such as a significant delay of the main rupture from the initial break and a slow source process, with an accuracy of about 10 to 20 sec.

Acknowledgments

We would like to thank Jeffrey Given, Fumiko Tajima, and Jeanne Sauber for helping us retrieve the seismograms from the GDSN day tapes. We thank Arthur Frankel for reviewing the manuscript. The IDA data used in this study were made available to us by courtesy of the IDA project team at the Institute of Geophysics and Planetary Physics, University of California, San Diego. This research was supported by NSF Grant EAR 811-6023 and USGS Contract 14-08-0001-21223. Division of Geological and Planetary Sciences, California Institute of Technology, Contribution Number 3922.

REFERENCES

Agnew, D., J. Berger, R. Buland, W. Farrell, and F. Gilbert (1976). International deployment of accelerometers: a network for very long period seismology, *EOS, Trans. Am. Geophys. Union* **57,** 180–188.

Aki, K. (1966). Generation and propagation of G waves from the Niigata earthquake of June 16, 1964. Part I. A statistical analysis, *Bull. Earthquake Res. Inst., Tokyo Univ.* **44,** 23–72.

Aki, K. and H. Patton (1978). Determination of seismic moment tensor using surface waves, *Tectonophysics* **49,** 213–222.

Ben-Menahem, A. (1961). Radiation of seismic surface waves from finite moving sources, *Bull. Seism. Soc. Am.* **51,** 401–435.

Boschi, E., F. Mulargia, E. Mantovani, M. Bonafede, A. M. Dziewonski, and J. H. Woodhouse (1981). The Irpinia earthquake of November 23, 1980, *EOS, Trans. Am. Geophys. Union* **62,** 330.

Cisternas, A., J. Dorel, and R. Gaulon (1982). Models of the complex source of the El Asnam earthquake, *Bull. Seism. Soc. Am.* **72,** 2245–2266.

Del Pezzo, E., G. Iannaccone, M. Martini, and R. Scarpa (1983). The 23 November 1980 southern Italy earthquake, *Bull. Seism. Soc. Am.* **73,** 187–200.

Deschamps, A., Y. Gaudemer, and A. Cisternas (1982). The El Asnam, Algeria, earthquake of 10 October 1980: multiple-source mechanism determined from long-period records, *Bull. Seism. Soc. Am.* **72,** 1111–1128.

Dziewonski, A. M. and J. H. Woodhouse (1983). An experiment in systematic study of global seismicity: Centroid-moment tensor solutions for 201 moderate and large earthquakes of 1981, *J. Geophys. Res.* **88,** 3247–3271.

Dziewonski, A. M., T.-A. Chou, and J. H. Woodhouse (1981). Determination of earthquake source parameters from waveform data for studies of global and regional seismicity, *J. Geophys. Res.* **86,** 2825–2852.

Eaton, J. P. (1981). Detailed study of the November 8, 1980, Eureka, Calif., earthquake and its aftershocks, *EOS, Trans. Am. Geophys. Union* **62,** 959.

Engdahl, E. R., J. Peterson, and N. A. Orsini (1982). Global digital network—current status and future directions, *Bull. Seism. Soc. Am.* **72,** S242–S259.

Furumoto, M. and I. Nakanishi (1983). Source times and scaling relations of large earthquakes, *J. Geophys. Res.* **88,** 2191–2198.

Geller, R. J. (1976). Scaling relations for earthquake source parameters and magnitudes, *Bull. Seism. Soc. Am.* **66,** 1501–1523.

Gilbert, F. (1981). An introduction to low-frequency seismology, in *Physics of the Earth's Interior*, A. M. Dziewonski and E. Boschi, Editors, North-Holland, Amsterdam, 41–81.

Gilbert, F. and A. M. Dziewonski (1975). An application of normal mode theory to the retrieval of structural parameters and source mechanisms from seismic spectra, *Phil. Trans. R. Soc. Lond., Ser. A* **278,** 187–269.

Hirn, A., H. Haessler, P. Hong Trong, G. Wittlinger, and L. A. Mendes Victor (1980). Aftershock sequence of the January 1st, 1980, earthquake and present-day tectonics in the Azores, *Geophys. Res. Letters* **7,** 501–504.

Julian, B. R. (1970). Ray tracing in arbitrarily heterogeneous media, *Lincoln Lab. Tech. Note* 1970–45.

Kanamori, H. and J. W. Given (1981). Use of long-period surface waves for rapid determination of earthquake-source parameters, *Phys. Earth Planet. Interiors* **27,** 8–31.

Kanamori, H. and J. W. Given (1982). Use of long-period surface waves for rapid determination of earthquake source parameters. 2. Preliminary determination of source mechanisms of large earthquakes ($M_s \geq 6.5$) in 1980, *Phys. Earth Planet. Interiors* **30,** 260–268.

King, G. C. P. and C. Vita-Finzi (1981). Active folding in the Algerian earthquake of 10 October 1980, *Nature* **292,** 22–26.

Lay, T., J. W. Given, and H. Kanamori (1982). Long-period mechanism of the 8 November 1980 Eureka, California, earthquake, *Bull. Seism. Soc. Am.* **72,** 439–456.

Mendiguren, J. A. and K. Aki (1978). Source mechanism of the deep Colombian earthquake of 1970 July 31 from the free oscillation data, *Geophys. J.* **55,** 539–556.

Nakanishi, I. and H. Kanamori (1982). Effects of lateral heterogeneity and source process time on the linear moment tensor inversion of long-period Rayleigh waves, *Bull. Seism. Soc. Am.* **72,** 2063–2080.

Oliver, J. and B. Isacks (1967). Deep earthquake zones, anomalous structures in the upper mantle, and the lithosphere, *J. Geophys. Res.* **72,** 4259–4275.

Ouyed, M., M. Megharaoui, A. Cisternas, A. Deschamps, J. Dorel, J. Frechet, R. Gaulon, D. Hatzfeld, and H. Philip (1981). Seismotectonics of the El Asnam earthquake, *Nature* **292,** 26–31.

Ouyed, M., G. Yielding, D. Hatzfeld, and G. C. P. King (1983). An aftershock study of the El Asnam (Algeria) earthquake of 1980 October 10, *Geophys. J.* **73,** 605–639.

Patton, H. (1980). Reference point equalization method for determining the source and path effects of surface waves, *J. Geophys. Res.* **85,** 821–848.

Romanowicz, B. (1981). Depth resolution of earthquakes in Central Asia by moment tensor inversion of long-period Rayleigh waves: effects of phase velocity variations across Eurasia and their calibration, *J. Geophys. Res.* **86,** 5963–5984.

Smith, S. W., R. C. McPherson, and N. I. Severy (1981). The Eureka earthquake of 1980, breakup of the Gorda plate, *Earthquake Notes* **52,** 44.

Solomon, S. C. and B. R. Julian (1974). Seismic constraints on ocean-ridge mantle structure: Anomalous fault-plane solutions from first motions, *Geophys. J.* **38,** 265–285.

Tajima, F. (1982). Study of seismic rupture pattern, *Ph.D. Thesis*, University of Tokyo, Tokyo, Japan.

Tajima, F. and H. Kanamori (1982). The July 1980 earthquake sequence in the Santa Cruz Islands, *EOS, Trans. Am. Geophys. Union* **63,** 385.

Toksöz, M. N., J. W. Minear, and B. R. Julian (1971). Temperature field and geophysical effects of a downgoing slab, *J. Geophys. Res.* **76,** 1113–1138.

Tréhu, A. M., J. L. Nábelek, and S. C. Solomon (1981). Source characterization of two Reykjanes ridge earthquakes: surface waves and moment tensors; *P* waveforms and nonorthogonal nodal planes, *J. Geophys. Res.* **86,** 1701–1724.

Utsu, T. (1967). Anomalies in seismic wave velocity and attenuation associated with a deep earthquake zone (I), *J. Fac. Sci. Hokkaido Univ., Ser. 7 (Geophys.)* **3,** 1–25.

Vidale, J. and H. Kanamori (1981). The October 1980 earthquake sequence in a seismic gap near the Loyalty Is., New Hebrides, *EOS, Trans. Am. Geophys. Union* **62,** 945.

SEISMOLOGICAL LABORATORY
CALIFORNIA INSTITUTE OF TECHNOLOGY
PASADENA, CALIFORNIA 91125

Manuscript received 12 August 1983